

# A Peristaltic Pump and Filter-Based Method for Aqueous Microplastic Sampling and Analysis

Zoë Harrold, Monica M. Arienzo,\* Meghan Collins, Julia M. Davidson, Xuelian Bai, Suja Sukumaran, and John Umek



Cite This: *ACS EST Water* 2022, 2, 268–277



Read Online

ACCESS |



Metrics & More



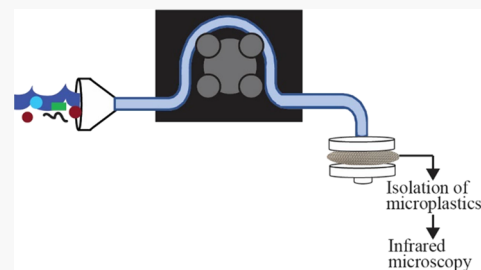
Article Recommendations



Supporting Information

**ABSTRACT:** Sampling the aquatic environment for microplastic concentration is inherently difficult because of variations in microplastic concentration, shape, and density and the potential for contamination. We present an assessment of a method for microplastic sampling that uses a peristaltic pump to pump water through a series of in-line stainless-steel mesh filters. Following filtration, the stainless-steel filters were treated using previously published methods to isolate microplastics, adjusted for the stainless-steel mesh filters. Microplastics were identified using micro-Fourier transform infrared ( $\mu$ FTIR) spectroscopy in transmission mode. This method was tested in the laboratory using standard polyethylene beads and was applied to two sample sites at the Las Vegas Wash in Nevada. The results showed that 70% of the polyethylene beads were recovered after the peristaltic pump and laboratory steps with minimal blank contamination. The advantages of the peristaltic pump sampling method are it (1) supports a range of sample volumes, (2) reduces sample handling, (3) reduces the potential for contamination, (4) provides flexibility in sampling locations, and (5) supports a variety of filter types. Using stainless-steel mesh filters allows for (1) streamlined and direct field-to-laboratory sample processing, (2)  $\mu$ FTIR transmission mode analysis of filter-mounted microplastics, and (3) reduced filter and sample processing costs.

**KEYWORDS:** microplastics, FTIR, freshwater, filter, peristaltic pump



## 1. INTRODUCTION

Synthetic plastic compounds were developed in the early 20th century, and widespread use of plastics began in the mid-20th century.<sup>1</sup> Microplastics (plastic particles with at least three dimensions  $\geq 1$  nm to  $\leq 5$  mm)<sup>2</sup> in particular are an emerging environmental concern because of their durability and small size. Recently, freshwaters have been found to contain substantial microplastic contamination, with rivers acting as a major conduit of microplastics to the marine environment.<sup>3–5</sup>

Sampling aquatic environments for microplastic concentration is inherently difficult because of the variations in microplastic concentration, shape, and density.<sup>6</sup> Many freshwater environments exhibit low microplastic concentrations, and therefore require a large sample volume.<sup>6</sup> For example, the American Society for Testing and Materials (ASTM)<sup>7</sup> recommends 1500 L for water samples with low to very low suspended solids. The complex sample matrix of freshwaters (e.g., algae, sediment, inorganic/organic materials, and biological materials) can interfere with and further complicate microplastic detection.<sup>8</sup> Low per liter microplastic concentrations also necessitate careful contamination control procedures both in the field and in the laboratory.<sup>9,10</sup> Lastly, the small size of microplastics requires sophisticated analytical approaches.<sup>8</sup> The ideal microplastic sampling approaches limit contamination while maximizing sample throughput and they are followed by laboratory methods that minimize sample

handling and contamination in the process of effectively isolating and identifying microplastic particles. This paper presents methods for sampling, laboratory processing, and analysis that address these needs.

Several sample collection procedures for microplastics in marine and freshwater environments have been presented in the existing literature (e.g., refs 6, 11, and 12). Net sampling and grab sampling are the most common microplastic sampling methods. Net sampling involves sampling the water surface using a neuston, bongo, or other types of plankton nets with a flow meter to determine the sample volume. The mesh is typically composed of nylon with a mesh size of 300  $\mu$ m, although some nets use a smaller mesh size (e.g., <100  $\mu$ m).<sup>3,11,13</sup> The net is typically designed to sample the top 0.5 m of water while it is pulled behind a boat<sup>14</sup> or held by individuals at the water surface.<sup>3</sup> After sample collection, the net is rinsed in a sample container and the material is stored until laboratory analysis. The primary benefit of the net method is it can filter large sample volumes (hundreds of liters), and

**Received:** July 30, 2021

**Revised:** January 6, 2022

**Accepted:** January 12, 2022

**Published:** January 31, 2022



therefore measure microplastics at low per liter concentrations. However, given the large surface area of the net, its plastic (i.e., nylon) makeup, and inevitable exposure to air, it is difficult to control for contamination. It is also challenging to ensure all particles are rinsed from the mesh into the sample container. The net can also entrain large debris (e.g., leaves and sticks) and become clogged in high-matrix environments.<sup>12</sup>

In contrast to net collection, the grab sampling approach<sup>4,15,16</sup> entails sampling waters with a container of known volume that is subsequently filtered in the lab. This method is limited by the volume of the sample container and the capability to carry multiple liters of water from each sample collection site. However, contamination can be controlled through filtration in a laboratory environment, and analysis is easier because there is less matrix material (e.g., sediment, algae, or other biological materials) than larger volume net samples. Previous studies comparing these two approaches noted that grab samples tend to exhibit higher microplastic counts per liter.<sup>4,16</sup>

Other microplastic sampling methods use portable pumps to pump water through stacked sieves,<sup>7,14,17–20</sup> in-line filters,<sup>21–23</sup> or into sample bottles.<sup>24</sup> These approaches allow for sample collection at various water depths, controlled sample collection volumes, and the option to vary the filter diameter and filter pore size.<sup>7,14,17,18,25</sup> When using stacked sieves, it may be difficult to control for contamination from atmospheric sources unless the sieves are covered with a non-plastic cover.<sup>18</sup> In contrast, the in-line filter approach isolates the water sample from the atmosphere (preventing potential contamination), but it may be subjected to contamination from pump tubing. Previous in-line filter approaches used a large, custom-built system,<sup>21,22</sup> involved backflushing filters into jars,<sup>19,26</sup> or involved backflushing onto alternative filters.<sup>23</sup> Therefore, there is a need to develop a portable (i.e., able to be carried in a backpack) and commercially available sampling approach that reduces sample handling and contamination potential (i.e., limits exposure to the atmosphere).

After freshwater sampling, the filtered material is brought back to the laboratory to isolate microplastic particles. This is typically conducted through a series of isolation and digestion steps.<sup>8,11,27–29</sup> Isolating microplastics from particulate matter is typically conducted using a dense (1.2 to 1.8 g/cm<sup>3</sup>) liquid (e.g., NaCl, ZnCl<sub>2</sub>, and CaCl<sub>2</sub>) that allows the plastic particles to float and the denser particulates to sink.<sup>8,11,27,28,30,31</sup> Care must be taken to choose a solution with an appropriate density for the plastics of interest.<sup>28</sup> For freshwater samples, an organic material is typically digested using an oxidizer and acid, base, and/or enzymatic digestion. These chemicals can dissolve or alter microplastics, and therefore they must be used with caution.<sup>11</sup> The microplastic isolation process may require multiple cycles of a given matrix-removal step or other separation processes.<sup>29</sup>

The size, shape, and polymer type of the microplastics can be determined once they are isolated from the sample matrix. Microplastic polymer identification approaches include infrared (IR) microscopy, Raman spectroscopy, pyrolysis-GC/MS, and visual identification to determine size, shape, and color. The identification approach used in this study was micro-Fourier transform IR ( $\mu$ FTIR) spectroscopy. Details on these other approaches can be found in the literature.<sup>8,32</sup> For  $\mu$ FTIR, the IR absorbance is dependent on the chemical properties of the plastic such that different plastic types produce unique spectra. This method is also nondestructive and collects magnified bright field images of the particles, making  $\mu$ FTIR an ideal approach for simultaneously identifying plastic type as well as particle size,

shape, and color. The  $\mu$ FTIR detects and analyzes plastic composition in particles down to  $\sim 10\ \mu\text{m}$ , while spatial mapping techniques acquire the spectra for all particles in a defined analytical area.

The material a sample is mounted on to is a critical consideration for  $\mu$ FTIR measurement. Many microplastic studies mount samples on filters, but many filters exhibit an absorbance that can interfere with or mask the IR transmission spectra of the sample.<sup>33</sup> Various filter options have been used for microplastic analysis—such as cellulose acetate, glass fiber, silicone, and polycarbonate filters—and users should consider the possible IR interferences for each filter type.<sup>34,35</sup> Filter costs also vary widely (<\$1 to >\$20 per filter), with silicone filters being more expensive.<sup>33</sup> Other approaches include selecting particles of interest and manually moving them from the filters to an IR transparent slide for analysis.<sup>10,36</sup> However, microplastics can be friable and statically charged, leading to broken and/or lost particles. One filter type that has been used for microplastic environmental sampling is stainless-steel mesh filters.<sup>21,23,36–40</sup> Other studies tested using stainless-steel mesh filters for organic matter digestion of the sample<sup>41</sup> or for the  $\mu$ FTIR identification of polymer type.<sup>42,43</sup> In this study, we built on that prior work by assessing the use of stainless-steel mesh filters for in-line sample filtration, laboratory processing, and  $\mu$ FTIR analysis in transmission mode for polymer identification.

Throughout these steps, care must be taken to eliminate potential contamination from sample handling, reagents, and exposure to the field and laboratory environment.<sup>8–10,28</sup> Best practices include ensuring the prefiltration of all reagents, carefully washing all laboratory glassware, positive control steps (cotton lab coats, clean air environments, etc.), and ensuring careful monitoring through regular blank assessments.<sup>6,9,10,28,44</sup>

To address the sampling, laboratory, and  $\mu$ FTIR analysis needs outlined above, we assessed a portable, field-deployable peristaltic pump with a series of in-line filters for microplastic sampling. We also tested the capability of stainless-steel mesh filters to isolate microplastics and for  $\mu$ FTIR identification of the polymer type. Our work demonstrated the applicability of the stainless-steel mesh for the entire sample life cycle, from sample collection to streamlining laboratory processing and subsequent  $\mu$ FTIR transmission mode sample mapping.

The methodology was subsequently tested in the laboratory using standard polyethylene (PE) beads and applied to the Las Vegas Wash (LVW) in Nevada, United States. The preliminary observations are presented herein. The LVW was selected to test these methods in the presence of a complex environmental sample matrix on waters of local and regional importance and in a location with microplastic data that were collected using other methods. Water in the LVW flows from Las Vegas into Lake Mead, which serves as a primary water source for neighboring states, recreation, and biota. Previous work demonstrated significant microparticle contamination of the water,<sup>45</sup> which is potentially because of the high anthropogenic use and input (including stormwater drainages and four wastewater treatment plants).<sup>45,46</sup>

## 2. METHODS

This section describes the (1) laboratory method used to assess the peristaltic pump approach, (2) method to isolate microplastics adjusted for the stainless-steel mesh filters, (3) laboratory blank assessment, (4) field application of the peristaltic pump and stainless-steel filter method, and (5)

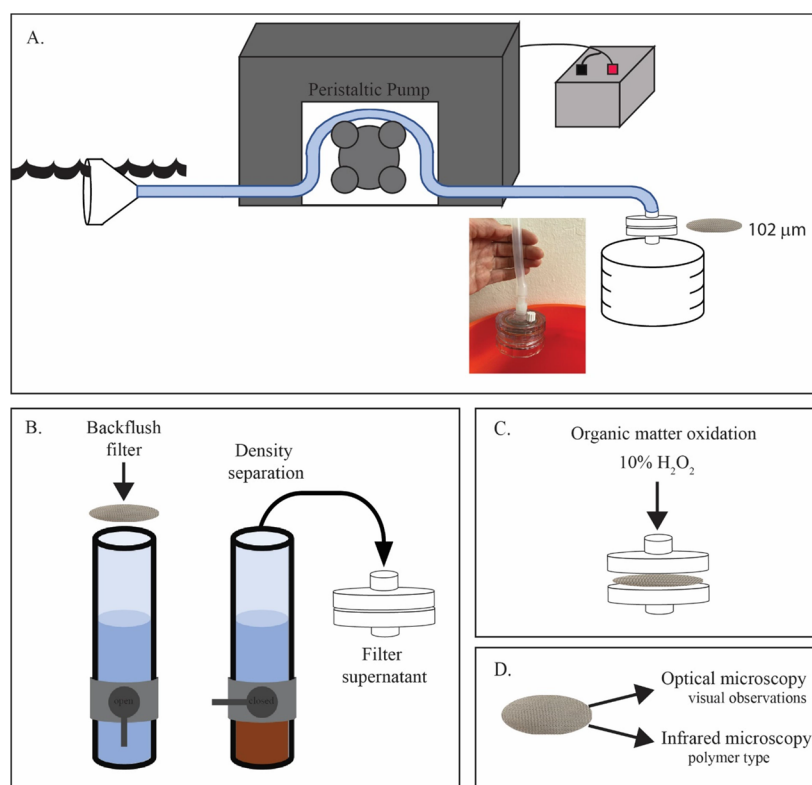


**Figure 1.** Peristaltic pumping (A) of water was followed by density separation (B), organic matter oxidation (C), and microscopy (D). Photo in (A) shows a 47 mm diameter filter housing.

**Table 1.** Count and Percent of the 125–150  $\mu\text{m}$  Polyethylene (PE) Beads Recovered for each Step: Peristaltic Pump (Pump), Zinc Chloride ( $\text{ZnCl}_2$ ) Density Separation, and Hydrogen Peroxide ( $\text{H}_2\text{O}_2$ ) Oxidation<sup>a</sup>

sample ID	initial count	pump volume (L)	pump count	pump % recovery	$\text{ZnCl}_2$ count	$\text{ZnCl}_2$ % recovery	$\text{H}_2\text{O}_2$ count	$\text{H}_2\text{O}_2$ % recovery	total % recovery
VMPS23	243	60	223.5	92	182	81	178	98	73
VMPS24	176	60	159	91	146	92	110	75	63
VMPS25	202	60	193.5	96	152	79	148	97	73
VMPS26	274	60	257	94	218	85	200	92	73
VMPS27	137	10	113	83					
VMPS28	151	10	119.5	79					
VMPS29	148	10	120	81					
VMPS21	370	60	316	85					
average				88		84		90	70
$\sigma$				6		6		10	5

<sup>a</sup>“Total recovery” is the total percent beads recovered from the initial count to the count after  $\text{H}_2\text{O}_2$  oxidation.

detection of stainless-steel filter-mounted microplastics using optical and IR microscopies.

**2.1. Peristaltic Pump and Filter Setup.** The peristaltic pump sampling method consists of a 230 mL funnel connected to silicone pump tubing (inner diameter: 6.35 mm; outer diameter: 11.12 mm; VWR, Wayne, Pennsylvania, United States) and the peristaltic pump (Figure 1A). The peristaltic pump is battery-operated (SERIES II Geopump, Geotech, Colorado, United States) and is fitted with a 60 to 600 rpm rotor. The in-line sample collection filters attach to the tubing outlet downstream of the pump (Figure 1A). The user has the flexibility to implement various filter types (e.g., different materials), filter diameters, and/or various filter pore sizes (in decreasing size fraction in the direction of the water flow). The volume of water that passes through the filter(s) can be measured to determine sample volume (Figure 1A).

**2.2. Peristaltic Pump Laboratory Test.** Particle losses may occur during field sampling, laboratory processing, and analysis regardless of the method used. Therefore, we used plastic beads to test microplastic recovery rates from the peristaltic pump sampling setup and laboratory processing method to help assess and account for microplastic losses.<sup>44</sup>

The peristaltic pump was set up as described above (section 2.1) and included one 47 mm diameter filter casing containing a stainless-steel mesh filter with a 102  $\mu\text{m}$  pore size connected in-line to the tubing outlet downstream of the pump (Figure 1A). We chose a 102  $\mu\text{m}$  stainless-steel mesh filter as this was similar in size to the 100  $\mu\text{m}$  neuston net used in previous studies.<sup>45</sup> Filters were composed of grade 304 stainless-steel mesh (TWP, California, United States) with a 66  $\mu\text{m}$  wire diameter and a 102  $\mu\text{m}$  mesh pore size. Filters were cut in-house to reduce costs and were precleaned by sonication prior to use. The filter was housed

in a polycarbonate filter casing (Pall Laboratory, New York, United States). We then used 125 to 150  $\mu\text{m}$  PE beads (Cospheric, Santa Barbara, CA) to test the plastic recovery. We placed PE beads onto weighing paper and precounted the beads using a Nikon SMZ1500 stereomicroscope. The beads were flushed into a funnel connected to the silicone peristaltic pump tubing. This was followed by flushing 5 to 55 L of filtered deionized water (5  $\mu\text{m}$  stainless-steel filter) from a spigot flowing to the mouth of the funnel and noting the total amount using a 20 L bucket with marked 5 L increments. Following the deionized water, we added 1 L of a filtered 0.5% solution of liquid cleaner (micro90, 0.7  $\mu\text{m}$  glass fiber, GF/F filter). The liquid cleaner was poured into the funnel and followed by 5 L of the filtered deionized water for a total of 10 to 60 L of water (Table 1). We then removed the stainless-steel filter from the filter casing, placed the filter in a petri dish (Pall Analyslide petri dish), and dried it at 40  $^{\circ}\text{C}$  for 8 to 12 h. To reduce potential contamination, the lid of the petri dish was kept loosely in place during the drying process. The dry stainless-steel filters were imaged (described in section 2.6), the PE beads were counted to determine the percent recovered from the peristaltic pump method, and the filter was stored in the dark until further laboratory processing. The silicone tubing was flushed with 60 L of filtered deionized water between samples.

**2.3. Isolation of Microplastics.** Similar to previous studies, we applied density separation and wet oxidation to remove particulate matter, oxidize organic materials, and isolate the microplastics.<sup>8,28</sup> These methods were adjusted for the stainless-steel filters to reduce the potential for contamination. Filters with standard PE beads (as described in section 2.2) were used to assess the recovery of microplastics at each step of the isolation process (Table 1). First, we conducted density separation and then conducted wet oxidation. The order of these steps can be interchangeable depending on the sample.

For density separation, we adopted a similar approach to Imhof et al.<sup>31</sup> and Coppock et al.<sup>47</sup> using zinc chloride ( $\text{ZnCl}_2$ ) and a separation column. The separation column was composed of a glass tube (Chemglass, Vineland, NJ, United States), a stainless-steel ball valve with silicone O-rings (McMaster Carr, Douglasville, GA, US) in the center of the glass tube, and a silicone stopper at the bottom of the glass tube (Figure 1B). The stainless-steel filter was removed from the petri dish and inverted into a stainless-steel funnel. Filtered  $\text{ZnCl}_2$  (0.7  $\mu\text{m}$  GF/F filter with a solution density of 1.5  $\text{g cm}^{-3}$ ) was used to backflush the material off the sample filter and into the separation column with the ball valve in the open position. We agitated the backflushed material for 5 min, allowed the sample to settle for 1 h, and repeated the 5 min agitation. The sample was then left undisturbed for 4 h to allow the denser particulate material to settle. After 4 h of settling, the ball valve was closed and the supernatant containing less dense particulates ( $<1.5 \text{ g cm}^{-3}$ ) was poured into a 250 mL funnel connected to a 47 mm polycarbonate filter housing containing the original backflushed filter. The glass separation column was rinsed with  $\text{ZnCl}_2$  twice followed by filtered deionized water to ensure the recovery of all materials. The filter housing was additionally rinsed with  $\sim 200$  mL of filtered deionized water to rinse the remaining  $\text{ZnCl}_2$  salts. The filter was removed from the filter housing, dried at 40  $^{\circ}\text{C}$  in the original petri dish, and subsequently imaged (see section 2.6). The PE beads were counted to assess the percent recovered after the  $\text{ZnCl}_2$  process, and the filter was stored in the dark until further laboratory processing.

To remove organic particles, the filter was placed inside a filter housing and the sample outlet port was plugged. Prefiltered (0.7  $\mu\text{m}$  glass fiber, GF/F filter) 10% hydrogen peroxide ( $\text{H}_2\text{O}_2$ ) was pipetted into the filter casing (Figure 1C) and the top of the filter casing was covered to prevent contamination. The filter was left for 12 to 24 h at room temperature ( $\sim 23$   $^{\circ}\text{C}$ ).  $\text{H}_2\text{O}_2$  was drained through the sample outlet port, and the filter was rinsed with filtered deionized water. The filter was removed from the filter housing, stored in the original petri dish, and dried at 40  $^{\circ}\text{C}$ . After drying, the stainless-steel filter was imaged and the PE beads were counted to assess the percent recovered after the  $\text{H}_2\text{O}_2$  wet oxidation process.

**2.4. Laboratory Blanks.** Laboratory blanks were prepared and analyzed for the peristaltic pump,  $\text{ZnCl}_2$  density separation, and  $\text{H}_2\text{O}_2$  wet oxidation steps. To assess potential contamination during the peristaltic pump step, 25 to 35 L of filtered deionized water followed by 1 L of 0.5% micro90 (0.7  $\mu\text{m}$  GF/F) and  $\sim 5$  L of filtered deionized water were passed through the peristaltic pump tubing and onto an in-line 102  $\mu\text{m}$  stainless-steel mesh filter. In total, this process took  $<2$  h to complete per sample. To assess potential contamination during density separation and wet oxidation, blank stainless-steel filters were processed in the same manner as the PE bead samples. All blank filters were dried and imaged using a microscope, and the particles were counted.

**2.5. Applying the Method to the Las Vegas Wash.** We applied the peristaltic pump and laboratory processing methods to two Las Vegas Wash sites (LVW04 and LVW05) sampled on September 13 and 14, 2019 (Figure 2 and Table S1). Similar to

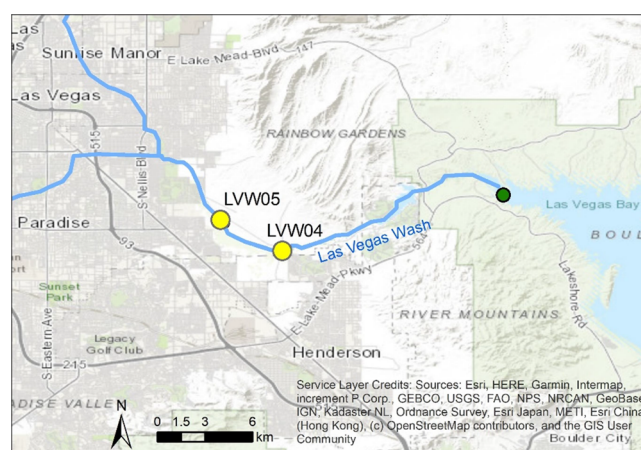


**Figure 2.** Map of the Las Vegas Wash (LVW). Yellow dots indicate sampling locations for this study and the green dot indicates the LVW sampling location from Baldwin et al.<sup>45</sup>

the setup described in section 2.1, we fitted the silicone peristaltic pump tubing inlet with a 250 mL polypropylene funnel to intake surface water by aligning the top of the funnel with the surface (e.g., sampling top  $\sim 0$ –5 cm) (Figure 1A). We secured the funnel to a rebar stake away from shoreline eddies approximately 3 to 4.5 m from the shoreline. Using the peristaltic pump, the tubing was flushed with  $\sim 20$  L of LVW surface water prior to installing the in-line filters. After flushing, three 25 mm diameter polypropylene (MilliporeSigma, Darmstadt, Germany) filter housings were connected in-line to the silicone tube outlet. Filter holders were prepared with 1 mm, 335  $\mu\text{m}$ , and 102  $\mu\text{m}$  stainless-steel filters from high to low size cutoffs along the direction of the flow. Water outflow was

collected in a bucket marked with 5 L increments to calculate the total volume for each filter. Filtration volumes were 27 and 30 L for LVW04 and LVW05, respectively (Table S1). Unlike in the laboratory tests, we did not rinse the tubing with the 0.5% micro90 solution, which was shown in the laboratory to increase standard PE bead recovery. At each site, sample filtration took <2 h to complete.

After sampling, the stainless-steel filters were kept in their filter housings, which were capped and stored in the refrigerator prior to laboratory processing. The filter housings were used as sample reaction vessels for the wet oxidation process. We filled the sealed filter casings with prefiltered 10% H<sub>2</sub>O<sub>2</sub> and allowed the filtered samples to oxidize for 24 h at room temperature, as described above. We drained and rinsed the stainless-steel filters with filtered deionized water. We then conducted the density separation for particulate matter removal (see the method outlined in section 2.3). After laboratory processing, the 102  $\mu\text{m}$  filters were oven-dried at 40 °C for at least 24 h. This study focused on the 102  $\mu\text{m}$  filters, which was the smallest size fraction collected and captured particles between 335 and 102  $\mu\text{m}$ . This size fraction most closely parallels the standard PE bead size (i.e., 125–150  $\mu\text{m}$ ) used to test method recovery. Data from the 1 mm and 335  $\mu\text{m}$  filters are not presented herein.

**2.6. Microscopy.** Optical microscopy was used to visually count the standard beads at each step of the process. We used a Nikon SMZ1500 stereo microscope coupled with an Olympus DP25 camera. We took images of the entire 47 mm stainless-steel sample filter at 20x magnification and stitched them together using Adobe Photoshop. Standard PE beads were counted twice by two individuals. The average difference between the two observers was 2.4 bead counts per filter, approximately 1.3% of the average bead count (Table 1). Laboratory blanks were treated in the same manner as samples and no difference in counts between the two observers was noted. The microplastic polymer type was identified using a Thermo Nicolet iN10 MX instrument housed at DRI. We analyzed the stainless-steel filters in transmission mode using the imaging detector mercury cadmium telluride (MCT)-cooled array with an aperture size of 25  $\mu\text{m}$   $\times$  25  $\mu\text{m}$  and step size of 25  $\mu\text{m}$ , a spectral resolution of 8  $\text{cm}^{-1}$  (from 4000 to 715  $\text{cm}^{-1}$ ), and a number of 64 scans. The Norton–Beer strong apodization function was applied by the instrument software. The background spectra using the same settings were automatically collected every 60 min. A previous study showed that mapping a filter at a 20 to 35  $\mu\text{m}$  step size and an aperture size of 50  $\mu\text{m}$   $\times$  50  $\mu\text{m}$  was adequate for detecting particles <100  $\mu\text{m}$ .<sup>48</sup> Results were corrected for baseline drift in the instrument software, and data were exported and processed using the Systematic Identification of MicroPLastics in the Environment (siMPLe) program.<sup>49–51</sup> The publicly available standard data set<sup>52</sup> was imported into the siMPLe and used to compare and identify the collected spectra. We tested the siMPLe program using known standard plastic materials and adjusted the threshold to match accordingly (Table S2). One randomly selected area of the VMPS25 standard (Table 1) with PE beads was analyzed, and two randomly selected areas of each LVW stainless-steel filter were analyzed to test the method.

**2.7. Contamination Reduction Procedures.** To reduce potential microplastic contamination, reagents were prefiltered using a Whatman 0.7  $\mu\text{m}$  GF/F filter and stored in glass containers. The laboratory deionized water was filtered using a 5  $\mu\text{m}$  stainless-steel filter. All laboratory ware, filter housings, and filters were cleaned with a filtered 1% micro90 solution (a

general cleaner), sonicated, and rinsed with filtered deionized water. The laboratory air was filtered using an MERV-13 filter. Cotton lab coats were required in the laboratory, and the laboratory working space, including bench tops and walls, were regularly wiped using a natural sponge or a lint-free wipe. Samples, laboratory glassware, and reagents were kept capped or covered with a heavy-duty aluminum foil whenever possible.

### 3. RESULTS AND DISCUSSION

**3.1. Laboratory Testing Results.** We counted the standard PE beads before and after each sample collection and treatment step (i.e., initial count, after peristaltic pump, after ZnCl<sub>2</sub>, and after H<sub>2</sub>O<sub>2</sub>). Results are shown as the percentage of beads recovered for each step and the total beads recovered throughout the process (Figure 3 and Table 1). On average,

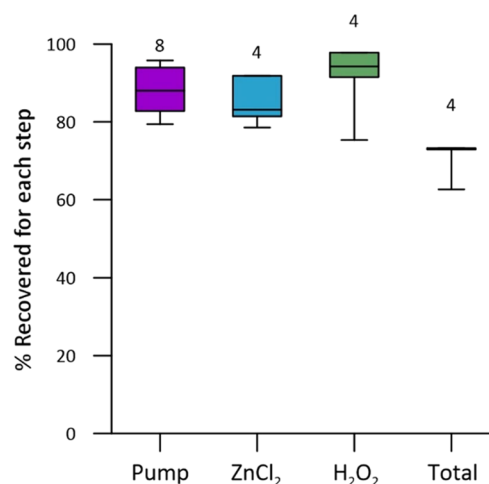


**Figure 3.** Percent of the polyethylene (PE) beads (125–150  $\mu\text{m}$  in size) recovered for each step. PE beads were counted before and after the peristaltic pump (Pump), zinc chloride (ZnCl<sub>2</sub>) density separation, and hydrogen peroxide (H<sub>2</sub>O<sub>2</sub>) oxidation steps. The percent of PE beads recovered was calculated for each step. The “Total” is the percent total beads recovered from the initial count relative to the final count after H<sub>2</sub>O<sub>2</sub> oxidation. Whiskers represent the 5/95 percentile and numbers above the whiskers are the *n* values.

88  $\pm$  6% (*n* = 8) of the PE beads were recovered from the peristaltic pump step. More PE beads were recovered during wet oxidation (90  $\pm$  10%, *n* = 4) than during density separation (84  $\pm$  6%, *n* = 4) (Figure 3), potentially because of the adherence of particles to the walls of the glass separation column used for density separation. In total, 70  $\pm$  5% of the PE beads were recovered.

Few previous studies have conducted plastic recovery assessments of each step of the laboratory process.<sup>10</sup> Lenz and Labrenz<sup>21</sup> tested a custom-built in-line filtration approach using polyamide particles that were 450 and 480  $\mu\text{m}$  in length and diameter, respectively. A recovery of 98.0  $\pm$  0.89% (*n* = 3) from the filtration process was observed. Similarly, Wang et al.<sup>53</sup> tested the filtration-based approach by pumping 100 particles ranging from 100  $\mu\text{m}$  to 6 mm through a 50  $\mu\text{m}$  steel sieve. The results showed a recovery of 92.7  $\pm$  4.5% (*n* = 3) plastic particles through the pumping system.<sup>53</sup> The results of the pumping system in this study were slightly lower (88  $\pm$  6%, *n* = 8), but the microplastic beads used were smaller on average than these previous studies, which may account for the difference. Simon et al.<sup>37</sup> added a known number of polystyrene beads (100  $\mu\text{m}$  in

size) to treated wastewater samples. The wastewater sample was then processed using a surfactant, cellulase enzymes, sieving, and  $\text{H}_2\text{O}_2$  and Fenton's reactions. Through this process,  $77.7 \pm 11.6\%$  of beads were recovered.<sup>37</sup> Vollertsen and Hansen<sup>54</sup> also added a known number of polystyrene beads ( $100 \mu\text{m}$  diameter) and high-density PE to raw wastewater. The water was treated with sodium dodecyl sulfate, cellulase, and  $\text{H}_2\text{O}_2$ . Recovery rates were  $78 \pm 17$  and  $61 \pm 29\%$  for polystyrene and high-density PE, respectively, from the wastewater samples.<sup>54</sup> Mintenig et al.<sup>20</sup> added PE beads ( $90$  to  $106 \mu\text{m}$ ) to  $1 \text{ L}$  of water and processed the positive control samples in the same manner as their river samples, which included adding sodium dodecyl sulfate, potassium hydroxide,  $\text{H}_2\text{O}_2$ , and  $\text{ZnCl}_2$  for separation. Results showed between a  $79.0$  and  $93.1\%$  recovery depending on the location of the sample preparation.<sup>20</sup> A total recovery of  $70 \pm 5\%$  of  $125$ – $150 \mu\text{m}$  standard PE beads in this study was similar to other published microplastic recovery rates.

Blank results showed minimal particle counts during the various steps (Tables S3 and S4). More particles were observed from the peristaltic pump and  $\text{ZnCl}_2$  blank (averages of  $4.8$  and  $4.3$  particles, respectively) when compared with the  $\text{H}_2\text{O}_2$  blank (average of  $0.8$  particles). The higher particle counts from the peristaltic pump blank was potentially because of the silicone tubing shedding microparticles, as supported by the dominance of translucent fragments observed in the peristaltic pump blanks (Table S5 and Figure S1). In addition to the translucent fragments, we observed red, blue, and black fibers and translucent films (Table S5). The California State Water Resources Control Board's<sup>2</sup> definition of microplastics includes silicone. A more resistant tubing or tubing made of a higher density polymer could be used (e.g., polytetrafluoroethylene, an average density of  $2.2 \text{ g cm}^{-3}$ ) so that if particles shed, they could be easily removed during density separation. Alternatively, the  $\mu\text{FTIR}$  spectra of the silicone tubing could be measured and compared with the samples. The increased  $\text{ZnCl}_2$  blank was potentially a result of this step requiring more handling of the sample (backflushing) and multiple rinses of the glass column that may have contributed to the increased blank. Combining this density separation method with the density separation approach presented by Mani et al.<sup>55</sup> could potentially reduce blank contamination.

Previous studies showed similar blank contributions. Wang et al.<sup>53</sup> tested the blank contribution of their pumping system and found  $0.33 \pm 0.58$  and  $0.67 \pm 0.58$  particles after pumping  $20 \text{ L}$  of distilled water through a  $50 \mu\text{m}$  sieve. Mintenig et al.<sup>20</sup> showed  $11.1$  particles per sample on average after laboratory processing of their blanks ( $1 \text{ L}$  of Milli-Q water) on the laboratory bench. Lower particles per sample were observed when samples were processed in the laminar flow hood.<sup>20</sup> Vermaire et al.<sup>56</sup> filtered  $100 \text{ L}$  of tap water through a  $100 \mu\text{m}$  filter, processed their blanks using  $\text{H}_2\text{O}_2$ , and identified  $0.02$  particles  $\text{L}^{-1}$ . Mintenig et al.<sup>23</sup> filtered blank water onto stainless-steel filter cartridges ( $124 \text{ mm}$  long) and found  $21$  particles per blank sample. The long polypropylene filter housings were thought to be the source of the contamination.<sup>23</sup> The plastic filter housings used in this study were not found to shed plastics, as observed in the previous study, but stainless-steel filter housings could be used, which range in cost from  $\$300$  to  $\$600$ . Alternatively, combining the approach presented here with the microplastic reactor approach<sup>38</sup> could also prevent contamination from the plastic housings.

To test the application of the stainless-steel filters to  $\mu\text{FTIR}$  spectroscopy, we imaged the stainless-steel filters with PE

standard beads that underwent laboratory processing. Using the siMPLe program, all the PE beads ( $125$ – $150 \mu\text{m}$ ) in the analysis area were identified on the  $102 \mu\text{m}$  stainless-steel mesh filter in transmission mode (Figure 4). The  $\mu\text{FTIR}$  spectroscopy results

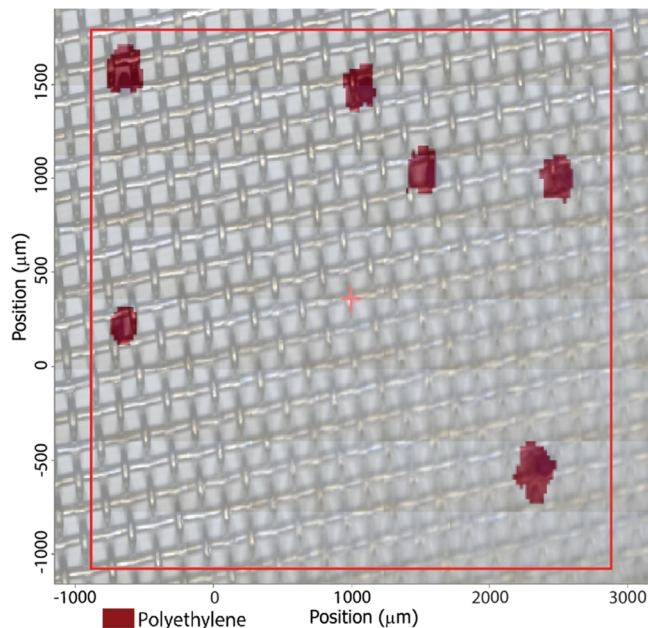


**Figure 4.** Micro-Fourier transform infrared ( $\mu\text{FTIR}$ ) identification of standard polyethylene (PE) beads of  $125$ – $150 \mu\text{m}$  in size on a stainless-steel filter with  $102 \mu\text{m}$  pore size. The mapped area was  $3.8 \text{ mm}$  by  $2.9 \text{ mm}$ . Axes show the scale in micrometers, and the red box shows the imaged area.  $\mu\text{FTIR}$  spectroscopy was conducted in transmission mode using the imaging array detectors, and the results were processed in siMPLe. Spectral results are overlain on the co-located optical image.

shown here further support the application of these filters in identifying microplastics in transmission mode, supporting previous applications of these types of filters.<sup>42,43</sup> These results are promising because previous studies either had to account for the IR absorbance of the filter (e.g., refs 35 and 49) or preselect putative microplastics using a light microscope followed by  $\mu\text{FTIR}$  measurement.<sup>10</sup> The stainless-steel mesh filters are therefore a valuable tool that addresses  $\mu\text{FTIR}$  analytical limitations and streamlines data collection for microplastic research.

**3.2. Las Vegas Wash.** The peristaltic pump and stainless-steel filter-based method for sampling and laboratory processing were tested by sampling LVW surface water at two locations. When conducting fieldwork, we minimized sample handling by keeping the filter in the housing until after the wet oxidation step that was conducted once we returned to the laboratory (see section 2.5). This approach further reduced potential particle loss and contamination by limiting filter handling.

Spectral analysis of the  $\mu\text{FTIR}$  data in siMPLe revealed polycarbonate, acrylate, and polypropylene in the analyzed areas of the LVW stainless-steel filters (Figure 5). These particles were primarily clear fragments, which made them difficult to detect with the optical microscope. The microplastics measured an average of  $187 \mu\text{m}$  in the major dimension and  $93 \mu\text{m}$  in the minor dimension (Table 2). The plastic types identified in this study were commonly observed in studies of surface waters from other rivers in urbanized areas.<sup>14,20,57–59</sup>

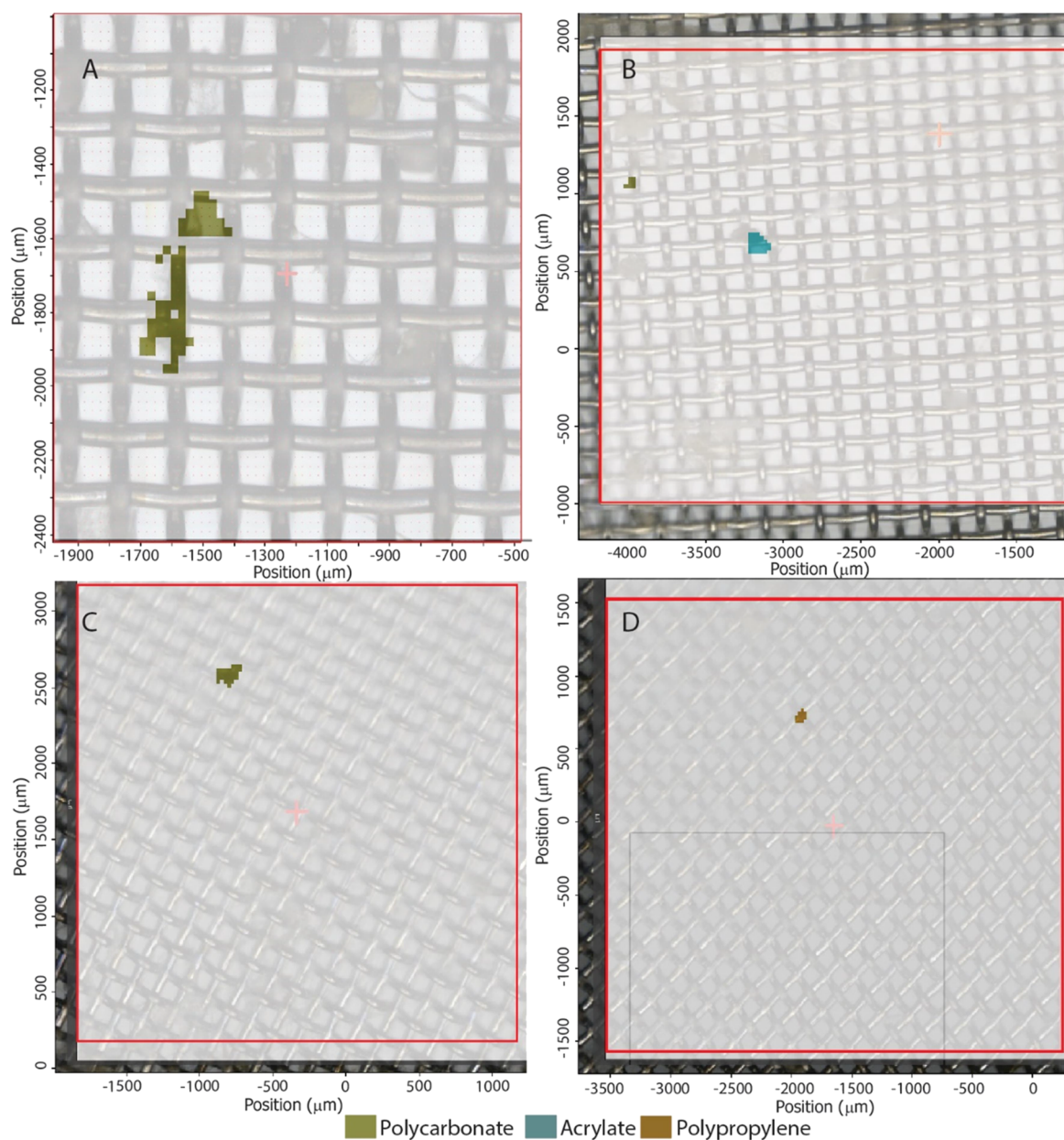


**Figure 5.** Las Vegas Wash (LVW) micro-Fourier transform infrared ( $\mu$ FTIR) spectroscopy results. Results from LVW04 from the two regions of the stainless-steel filter ( $102\ \mu\text{m}$  opening) are shown in (A) and (B). Imaged area sizes are 1.5 by 1.43 mm for (A) and 3 by 2.9 mm for (B). Results from LVW05 from the two regions of the stainless-steel filter ( $102\ \mu\text{m}$  opening) are shown in (C) and (D). Imaged area sizes are 3 by 3.4 mm for (C) and 3.7 by 3.1 mm for (D). Axes show the scale in micrometers and the red box shows the imaged area.  $\mu$ FTIR spectroscopy was conducted in transmission mode using the imaging array detectors and results were processed in siMPle. Spectral results are overlain on the co-located optical image.

**Table 2.** Characteristics of Polymers Identified by siMPle from the Las Vegas Wash

site	identifier	polymer <sup>a</sup>	major dimension ( $\mu\text{m}$ ) <sup>a</sup>	minor dimension ( $\mu\text{m}$ ) <sup>a</sup>	color	shape
LVW04	1	polycarbonate	352.4	97.1	transparent	fragment
LVW04	2	polycarbonate	177.1	98.9	transparent	fragment
LVW04	3	polycarbonate	95.7	58.2	transparent	fragment
LVW04	4	acrylate	185.1	124.7	black	fragment
LVW05	1	polycarbonate	199	108	translucent	fragment
LVW05	2	polypropylene	115.1	76	transparent	fragment

<sup>a</sup>Determined using the siMPle program.

Baldwin et al.<sup>45</sup> measured microparticle contamination of the LVW using a  $100\ \mu\text{m}$  neuston net from one LVW site located much closer to the Las Vegas Bay (Figure 2). Their findings

indicated high microparticle contamination at the Las Vegas Bay site ( $9.7\ \text{particles m}^{-3}$ ), but spectroscopic methods were not used to measure the plastic type.<sup>45</sup> Rather, the particle shape

(e.g., foam, film, fiber, bead, or fragment) was used to categorize the microparticles observed.<sup>45</sup> Baldwin et al.<sup>45</sup> showed a diversity of microparticle shapes from LVW water samples, with the dominant shape being fibers. In our study, the siMPle program did not identify microplastic fibers. Additional  $\mu$ FTIR and microplastic morphology (i.e., size, shape, and color) analyses of the LVW sample filters are needed to compare our data with the Baldwin et al.<sup>45</sup> results.

#### 4. CONCLUSIONS

The method for microplastic field sampling used in this study is portable and easy to use. The peristaltic pump method uses commercially available products that do not require customization. The peristaltic pump method is adaptable to numerous sampling locations (e.g., freshwater, remote and hard-to-access locations, as well as shore-based and surface sampling, and it is potentially adaptable to seawater, boat-based, and depth sampling). It also supports various in-line filter types and sizes, is relatively inexpensive (approximate costs in US dollars are \$1300 for the pump, \$20 for a rechargeable battery, \$200 for pump tubing, and \$18 for the in-line filter housing), and can filter 100 L in  $\sim$ 3 h. These factors make this method applicable to a range of sampling locations and sample types. Additionally, we observed high particle recovery (88%) and minimal blank contribution during laboratory testing of the peristaltic pump sampling method. The potential limitations of peristaltic pump sampling include shedding of the silicone pump tubing and clogging of the filters in waters with high matrix materials.

The stainless-steel filters provide a streamlined approach for the entire microplastic sampling process from sample collection and laboratory processing to  $\mu$ FTIR spectroscopic analysis. Storing stainless-steel filters in the filter housing prior to laboratory processing further limits sample handling, and the filter housings are suitable vessels for the wet oxidation digestion processes. The stainless-steel filters also support streamlined laboratory processing in part because of their resistance to corrosion during  $H_2O_2$  and  $ZnCl_2$  treatments. The reduced sample handling also reduces particle loss during laboratory processing—on average 90% PE bead recovery during  $H_2O_2$  and 84% PE bead recovery during density separation. The low-cost ( $\sim$ \$1 per filter) stainless-steel filters are affordable, easy to decontaminate, and potentially adaptable to other processing steps (such as enzymatic digestion<sup>29,38</sup>) and for other sample types (e.g., ocean water, biota,<sup>40</sup> or wastewater) (not shown here). Lastly, the 102  $\mu$ m mesh stainless-steel filters are suitable as a sample-mounting substrate for  $\mu$ FTIR in transmission mode. The 102  $\mu$ m mesh pore size is relatively large, but the availability of smaller (e.g., 20  $\mu$ m) mesh pore sizes<sup>23,37,38</sup> is promising for studying smaller microplastics, although the lower limit of stainless-steel mesh pore size is  $\sim$ 20  $\mu$ m. In summary, the peristaltic pump and stainless-steel mesh filters are promising for microplastic sampling, laboratory processing, and analysis and have the potential to be used for a variety of sample types and locations.

#### ■ ASSOCIATED CONTENT

##### SI Supporting Information

The Supporting Information is available free of charge at <https://pubs.acs.org/doi/10.1021/acsestwater.1c00270>.

(Tables S1–S5 and Figure S1) Sample locations, thresholds used for various materials, and blank results (PDF)

#### ■ AUTHOR INFORMATION

##### Corresponding Author

Monica M. Arienzo – Desert Research Institute Reno, Reno, Nevada 89512, United States; [orcid.org/0000-0003-3444-9810](https://orcid.org/0000-0003-3444-9810); Phone: 775-673-7693; Email: [marienzo@dri.edu](mailto:marienzo@dri.edu)

##### Authors

Zoë Harrold – Desert Research Institute Reno, Reno, Nevada 89512, United States; Clear Horizons Consulting, Sparks, Nevada 89431, United States

Meghan Collins – Desert Research Institute Reno, Reno, Nevada 89512, United States

Julia M. Davidson – Desert Research Institute Reno, Reno, Nevada 89512, United States; University of Nevada, Reno, Reno, Nevada 89557, United States

Xuelian Bai – Desert Research Institute Las Vegas, Las Vegas, Nevada 89119, United States

Suja Sukumaran – Thermo Fisher Scientific, San Jose, California 95134, United States

John Umek – Desert Research Institute Reno, Reno, Nevada 89512, United States

Complete contact information is available at:

<https://pubs.acs.org/10.1021/acsestwater.1c00270>

##### Notes

The authors declare no competing financial interest.

#### ■ ACKNOWLEDGMENTS

We would like to acknowledge the two reviewers whose comments improved the manuscript. Additionally, we would like to thank Nicole Damon for her comments on the manuscript. Funding for method development and field sampling was provided by the DRI Foundation to M.M.A., Z.H., and M.C. Additional internal DRI funds were provided to M.M.A., Z.H., M.C., and X.B. for method development and field sampling in the Las Vegas Wash. Maki Endowment funds were provided to M.M.A., J.U., and Z.H. for field sampling and method validation. Additional funding was provided by NSF grants 2018848 and 2045871 to M.M.A. Data are available at <https://doi.org/10.5061/dryad.12jm63xz4>.

#### ■ REFERENCES

- (1) Geyer, R.; Jambeck, J. R.; Law, K. L. Production, Use, and Fate of All Plastics Ever Made. *Sci. Adv.* **2017**, *3*, No. e1700782.
- (2) California State Water Resources Control Board Proposed Definition of Microplastics in Drinking Water; 2020.
- (3) Baldwin, A. K.; Corsi, S. R.; Mason, S. A. Plastic Debris in 29 Great Lakes Tributaries: Relations to Watershed Attributes and Hydrology. *Environ. Sci. Technol.* **2016**, *50*, 10377–10385.
- (4) Kapp, K. J.; Yeatman, E. Microplastic Hotspots in the Snake and Lower Columbia Rivers: A Journey from the Greater Yellowstone Ecosystem to the Pacific Ocean. *Environ. Pollut.* **2018**, *241*, 1082–1090.
- (5) Skalska, K.; Ockelford, A.; Ebdon, J. E.; Cundy, A. B. Riverine Microplastics: Behaviour, Spatio-Temporal Variability, and Recommendations for Standardised Sampling and Monitoring. *Journal of Water Process Engineering* **2020**, *38*, 101600.
- (6) Brander, S. M.; Renick, V. C.; Foley, M. M.; Steele, C.; Woo, M.; Lusher, A.; Carr, S.; Helm, P.; Box, C.; Cherniak, S.; Andrews, R. C.; Rochman, C. M. Sampling and Quality Assurance and Quality Control: A Guide for Scientists Investigating the Occurrence of Microplastics Across Matrices. *Appl. Spectrosc.* **2020**, *74*, 1099–1125.
- (7) ASTM D8332–20. *Standard Practice for Collection of Water Samples with High, Medium, or Low Suspended Solids for Identification*



and Quantification of Microplastic Particles and Fibers; ASTM International: West Conshohocken, PA, 2020, DOI: 10.1520/D8332-20.

(8) GESAMP Guidelines for the Monitoring and Assessment of Plastic Litter in the Ocean; Kershaw, P.; Turra, A.; Galgani, F., Eds.; United Nations Environment Programme (UNEP): 2019.

(9) Hermsen, E.; Mintenig, S. M.; Besseling, E.; Koelmans, A. A. Quality Criteria for the Analysis of Microplastic in Biota Samples: A Critical Review. *Environ. Sci. Technol.* **2018**, *52*, 10230–10240.

(10) Koelmans, A. A.; Nor, N. H. M.; Hermsen, E.; Kooi, M.; Mintenig, S. M.; De France, J. Microplastics in Freshwaters and Drinking Water: Critical Review and Assessment of Data Quality. *Water Res.* **2019**, *155*, 410–422.

(11) Stock, F. B.; Narayana, V. K.; Scherer, C.; Löder, M. G. J.; Brennholt, N.; Laforsch, C.; Reifferscheid, G. *Pitfalls and Limitations in Microplastic Analyses*; Springer Berlin Heidelberg: Berlin, Heidelberg, 2020, pp. 1–30, DOI: 10.1007/978\_2020\_654.

(12) Klein, S.; Dimzon, I. K.; Eubeler, J.; Knepper, T. P. Analysis, Occurrence, and Degradation of Microplastics in the Aqueous Environment. In *Freshwater microplastics*; Springer: Cham, 2018, pp. 51–67.

(13) Conkle, J. L.; Báez Del Valle, C. D.; Turner, J. W. Are We Underestimating Microplastic Contamination in Aquatic Environments? *Environ. Manage.* **2018**, *61*, 1–8.

(14) Sutton, R.; Franz, A.; Gilbreath, A.; Lin, L.; Miller, M.; Sedlak, A.; Wong, A.; Box, C.; Holleman, R.; Munno, K.; Zhu, X. *Understanding Microplastic Levels, Pathways, and Transport in the San Francisco Bay Region*; San Francisco Estuary Institute: 2019.

(15) Dubaish, F.; Liebezeit, G. Suspended Microplastics and Black Carbon Particles in the Jade System, Southern North Sea. *Water, Air, Soil Pollut.* **2013**, *224*, 1352.

(16) Barrows, A. P. W.; Neumann, C. A.; Berger, M. L.; Shaw, S. D. Grab vs. Neuston Tow Net: A Microplastic Sampling Performance Comparison and Possible Advances in the Field. *Anal. Methods* **2017**, *9*, 1446–1453.

(17) Wang, W.; Ndungu, A. W.; Li, Z.; Wang, J. Microplastics Pollution in Inland Freshwaters of China: A Case Study in Urban Surface Waters of Wuhan, China. *Sci. Total Environ.* **2017**, *575*, 1369–1374.

(18) Tamminga, M.; Stoewer, S.-C.; Fischer, E. K. On the Representativeness of Pump Water Samples versus Manta Sampling in Microplastic Analysis. *Environ. Pollut.* **2019**, *254*, 112970.

(19) Zhang, L.; Liu, J.; Xie, Y.; Zhong, S.; Yang, B.; Lu, D.; Zhong, Q. Distribution of Microplastics in Surface Water and Sediments of Qin River in Beibu Gulf, China. *Sci. Total Environ.* **2020**, *708*, 135176.

(20) Mintenig, S. M.; Kooi, M.; Erich, M. W.; Primpke, S.; Redondo-Hasselerharm, P. E.; Dekker, S. C.; Koelmans, A. A.; van Wezel, A. P. A Systems Approach to Understand Microplastic Occurrence and Variability in Dutch Riverine Surface Waters. *Water Res.* **2020**, *176*, 115723.

(21) Lenz, R.; Labrenz, M. Small Microplastic Sampling in Water: Development of an Encapsulated Filtration Device. *Water* **2018**, *10*, 1055.

(22) Pittroff, M.; Müller, Y. K.; Witzig, C. S.; Scheurer, M.; Storck, F. R.; Zumbülte, N. Microplastic Analysis in Drinking Water Based on Fractionated Filtration Sampling and Raman Microspectroscopy. *Environ. Sci. Pollut. Res.* **2021**, *28*, 59439–59451.

(23) Mintenig, S. M.; Int-Veen, I.; Löder, M. G. J.; Primpke, S.; Gerdts, G. Identification of Microplastic in Effluents of Waste Water Treatment Plants Using Focal Plane Array-Based Micro-Fourier-Transform Infrared Imaging. *Water Res.* **2017**, *108*, 365–372.

(24) Martin, K. M.; Hasenmueller, E. A.; White, J. R.; Chambers, L. G.; Conkle, J. L. Sampling, Sorting, and Characterizing Microplastics in Aquatic Environments with High Suspended Sediment Loads and Large Floating Debris. *JoVE* **2018**, *137*, 57969.

(25) Di, M.; Wang, J. Microplastics in Surface Waters and Sediments of the Three Gorges Reservoir, China. *Sci. Total Environ.* **2018**, *616*–617, 1620–1627.

(26) Zheng, Y.; Li, J.; Sun, C.; Cao, W.; Wang, M.; Jiang, F.; Ju, P. Comparative Study of Three Sampling Methods for Microplastics Analysis in Seawater. *Sci. Total Environ.* **2021**, *765*, 144495.

(27) Masura, J.; Baker, J. E.; Foster, G. D.; Arthur, C.; Herring, C. *Laboratory Methods for the Analysis of Microplastics in the Marine Environment: Recommendations for Quantifying Synthetic Particles in Waters and Sediments*; Marine Debris Program (U.S.) Ed.; NOAA Marine Debris Division Silver Spring, MD: NOAA technical memorandum NOS-OR&R: 48; 2015.

(28) Lusher, A. L.; Munno, K.; Hermabessiere, L.; Carr, S. Isolation and Extraction of Microplastics from Environmental Samples: An Evaluation of Practical Approaches and Recommendations for Further Harmonization. *Appl. Spectrosc.* **2020**, *74*, 1049–1065.

(29) ASTM D8333–20. *Standard Practice for Preparation of Water Samples with High, Medium, or Low Suspended Solids for Identification and Quantification of Microplastic Particles and Fibers Using Raman Spectroscopy, IR Spectroscopy, or Pyrolysis-GC/MS*; ASTM International: West Conshohocken, PA, 2020, DOI: 10.1520/D8333-20.

(30) Hidalgo-Ruz, V.; Gutow, L.; Thompson, R. C.; Thiel, M. Microplastics in the Marine Environment: A Review of the Methods Used for Identification and Quantification. *Environ. Sci. Technol.* **2012**, *46*, 3060–3075.

(31) Imhof, H. K.; Schmid, J.; Niessner, R.; Ivleva, N. P.; Laforsch, C. A Novel, Highly Efficient Method for the Separation and Quantification of Plastic Particles in Sediments of Aquatic Environments. *Limnology and Oceanography: Methods* **2012**, *10*, 524–537.

(32) Li, J.; Liu, H.; Chen, J. P. Microplastics in Freshwater Systems: A Review on Occurrence, Environmental Effects, and Methods for Microplastics Detection. *Water Res.* **2018**, *137*, 362–374.

(33) Primpke, S.; Christiansen, S. H.; Cowger, W.; De Frond, H.; Deshpande, A.; Fischer, M.; Holland, E. B.; Meyns, M.; O'Donnell, B. A.; Ossmann, B. E.; Pittroff, M.; Sarau, G.; Scholz-Böttcher, B. M.; Wiggan, K. J. Critical Assessment of Analytical Methods for the Harmonized and Cost-Efficient Analysis of Microplastics. *Appl. Spectrosc.* **2020**, *74*, 1012–1047.

(34) Käßler, A.; Windrich, F.; Löder, M. G. J.; Malanin, M.; Fischer, D.; Labrenz, M.; Eichhorn, K.-J.; Voit, B. Identification of Microplastics by FTIR and Raman Microscopy: A Novel Silicon Filter Substrate Opens the Important Spectral Range below 1300  $\text{cm}^{-1}$  for FTIR Transmission Measurements. *Anal. Bioanal. Chem.* **2015**, *407*, 6791–6801.

(35) Löder, M. G. J.; Kuczera, M.; Mintenig, S.; Lorenz, C.; Gerdts, G. Focal Plane Array Detector-Based Micro-Fourier-Transform Infrared Imaging for the Analysis of Microplastics in Environmental Samples. *Environ. Chem.* **2015**, *12*, 563.

(36) Feld, L.; Silva, V. H. d.; Murphy, F.; Hartmann, N. B.; Strand, J. A Study of Microplastic Particles in Danish Tap Water. *Water* **2021**, *13*, 2097.

(37) Simon, M.; van Alst, N.; Vollertsen, J. Quantification of Microplastic Mass and Removal Rates at Wastewater Treatment Plants Applying Focal Plane Array (FPA)-Based Fourier Transform Infrared (FT-IR) Imaging. *Water Res.* **2018**, *142*, 1–9.

(38) Lorenz, C.; Roscher, L.; Meyer, M. S.; Hildebrandt, L.; Prume, J.; Löder, M. G. J.; Primpke, S.; Gerdts, G. Spatial Distribution of Microplastics in Sediments and Surface Waters of the Southern North Sea. *Environ. Pollut.* **2019**, *252*, 1719–1729.

(39) Strand, J.; Feld, L.; Murphy, F.; Mackevica, A.; Hartmann, N. B. *Analysis of Microplastic Particles in Danish Drinking Water*; DCE-Danish Centre for Environment and Energy: 2018.

(40) Dawson, A. L.; Motti, C. A.; Kroon, F. J. Solving a Sticky Situation: Microplastic Analysis of Lipid-Rich Tissue. *Front. Environ. Sci.* **2020**, *8*, 163.

(41) Löder, M. G. J.; Imhof, H. K.; Ladehoff, M.; Löschel, L. A.; Lorenz, C.; Mintenig, S.; Piehl, S.; Primpke, S.; Schrank, I.; Laforsch, C.; Gerdts, G. Enzymatic Purification of Microplastics in Environmental Samples. *Environ. Sci. Technol.* **2017**, *51*, 14283–14292.

(42) Xu, J.-L.; Hassellöv, M.; Yu, K.; Gowen, A. A. Microplastic Characterization by Infrared Spectroscopy. *Handbook of Microplastics in the Environment* **2020**, 1–33.

(43) Xu, J.-L.; Thomas, K. V.; Luo, Z.; Gowen, A. A. FTIR and Raman Imaging for Microplastics Analysis: State of the Art, Challenges and Prospects. *TrAC Trends Anal. Chem.* **2019**, *119*, 115629.

(44) Cowger, W.; Booth, A.; Hamilton, B.; Primpke, S.; Munno, K.; Lusher, A.; Dehaut, A.; Vaz, V. P.; Liboiron, M.; Devriese, L. I. EXPRESS: Reporting Guidelines to Increase the Reproducibility and Comparability of Research on Microplastics. *Appl. Spectrosc.* **2020**, *74*, 1066.

(45) Baldwin, A. K.; Spanjer, A. R.; Rosen, M. R.; Thom, T. Microplastics in Lake Mead National Recreation Area, USA: Occurrence and Biological Uptake. *PLoS One* **2020**, *15*, No. e0228896.

(46) Gautam, M.; Acharya, K.; Shanahan, S. A. Ongoing Restoration and Management of Las Vegas Wash: An Evaluation of Success Criteria. *Water Policy* **2014**, *16*, 720–738.

(47) Coppock, R. L.; Cole, M.; Lindeque, P. K.; Queirós, A. M.; Galloway, T. S. A Small-Scale, Portable Method for Extracting Microplastics from Marine Sediments. *Environ. Pollut.* **2017**, *230*, 829–837.

(48) Mintenig, S. M.; Bäuerlein, P. S.; Koelmans, A. A.; Dekker, S. C.; van Wezel, A. P. Closing the Gap between Small and Smaller: Towards a Framework to Analyse Nano- and Microplastics in Aqueous Environmental Samples. *Environ. Sci.: Nano* **2018**, *5*, 1640–1649.

(49) Primpke, S.; Lorenz, C.; Rascher-Friesenhausen, R.; Gerdts, G. An Automated Approach for Microplastics Analysis Using Focal Plane Array (FPA) FTIR Microscopy and Image Analysis. *Anal. Methods* **2017**, *9*, 1499–1511.

(50) Primpke, S.; Dias, P. A.; Gerdts, G. Automated Identification and Quantification of Microfibres and Microplastics. *Anal. Methods* **2019**, *11*, 2138–2147.

(51) Primpke, S.; Cross, R. K.; Mintenig, S. M.; Simon, M.; Vianello, A.; Gerdts, G.; Vollertsen, J. Toward the Systematic Identification of Microplastics in the Environment: Evaluation of a New Independent Software Tool (SiMPle) for Spectroscopic Analysis. *Appl. Spectrosc.* **2020**, *74*, 1127–1138.

(52) Primpke, S.; Wirth, M.; Lorenz, C.; Gerdts, G. Reference Database Design for the Automated Analysis of Microplastic Samples Based on Fourier Transform Infrared (FTIR) Spectroscopy. *Anal. Bioanal. Chem.* **2018**, *410*, 5131–5141.

(53) Wang, W.; Yuan, W.; Chen, Y.; Wang, J. Microplastics in Surface Waters of Dongting Lake and Hong Lake, China. *Sci. Total Environ.* **2018**, *633*, 539–545.

(54) Vollertsen, J.; Hansen, A. A. *Microplastic in Danish Wastewater: Sources, Occurrences and Fate*; The Danish Environmental Protection Agency: 2017.

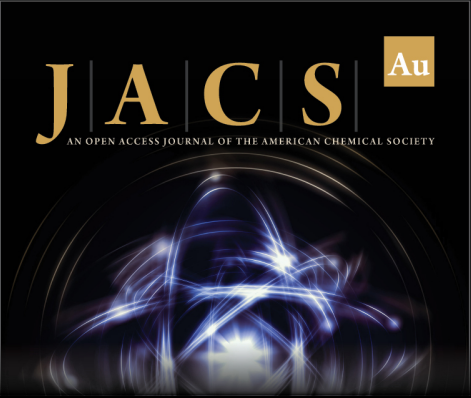
(55) Mani, T.; Primpke, S.; Lorenz, C.; Gerdts, G.; Burkhardt-Holm, P. Microplastic Pollution in Benthic Midstream Sediments of the Rhine River. *Environ. Sci. Technol.* **2019**, *53*, 6053–6062.

(56) Vermaire, J. C.; Pomeroy, C.; Herczegh, S. M.; Haggart, O.; Murphy, M. Microplastic Abundance and Distribution in the Open Water and Sediment of the Ottawa River, Canada, and Its Tributaries. *FACETS* **2017**, *2*, 301–314.


(57) Mani, T.; Hauk, A.; Walter, U.; Burkhardt-Holm, P. Microplastics Profile along the Rhine River. *Sci. Rep.* **2016**, *5*, 17988.

(58) Campanale, C.; Stock, F.; Massarelli, C.; Kochleus, C.; Bagnuolo, G.; Reifferscheid, G.; Uricchio, V. F. Microplastics and Their Possible Sources: The Example of Ofanto River in Southeast Italy. *Environ. Pollut.* **2020**, *258*, 113284.


(59) Schwarz, A. E.; Ligthart, T. N.; Boukris, E.; van Harmelen, T. Sources, Transport, and Accumulation of Different Types of Plastic Litter in Aquatic Environments: A Review Study. *Mar. Pollut. Bull.* **2019**, *143*, 92–100.




**JACS** Au  
AN OPEN ACCESS JOURNAL OF THE AMERICAN CHEMICAL SOCIETY



Editor-in-Chief  
**Prof. Christopher W. Jones**  
Georgia Institute of Technology, USA

**Open for Submissions** 

pubs.acs.org/jacsau  ACS Publications  
Most Trusted. Most Cited. Most Read.